A novel strategy for making soluble reduced graphene oxide sheets cheaply by adopting an endogenous reducing agent†

Kelong Ai,[a] Yanlan Liu,[ab] Lehui Lu,*[a] Xiaoli Cheng[c] and Lihua Huo[c]

Received 30th August 2010, Accepted 16th October 2010
DOI: 10.1039/c0jm02865g

A facile and efficient strategy is described for the fabrication of soluble reduced graphene oxide (rGO) sheets. Different from the conventional strategies, the proposed method is based on the reduction of graphene oxide by an endogenous reducing agent from a most widely used and cost-effective solvent, without adding any other toxic reducing agent. Simultaneously, this solvent can serve as an effective stabilizer, avoiding complicated and time-consuming modification procedures. The as-prepared rGO sheets not only exhibit high reduction level and conductivity, but also can be well dispersed in many solvents. Of particular significance is that rGO sheets can be produced in large quantities. These advantages endow this proposed synthetic approach great potential applications in the construction of high-performance graphene-based devices at low cost, as demonstrated in our study of NO gas sensing.

1. Introduction

Fabrication of graphene sheets is actively pursued for applications in nanoelectronics, sensors, nanocomposites, batteries, supercapacitors and hydrogen storage.[1] Central to these efforts is a drive to search for an efficient approach to large-scale production of processable graphene sheets at a relatively low cost. For established procedures such as chemical vapour deposition, ultrasonic exfoliation or mechanical exfoliation, obtaining graphene sheets in large quantities is still a big challenge.[2] An alternative strategy based on the reduction of graphene oxide (GO) has moved into spotlight at present owing to readily available precursors, significant advantages with wet chemical synthesis and high yield.[3] Furthermore, there is a crucial point for preparing graphene sheets which must first be considered, that is the dispersion of the as-prepared graphene sheets in different solvents, because many practical applications require them to be processed in solution phase.[4] Unfortunately, graphene sheets suffer from aggregation resulting from strong Van der Waals attractive forces between the graphene planes in solvent without recourse to special stabilizers, which brings out a great technical obstacle in graphene practical applications.

Nowadays, two typical strategies have been developed to address these issues for producing soluble and large-scale rGO sheets using GO as the precursor. In the first strategy, GO was firstly reduced by certain reducing agents, followed by covalently or noncovalently functionalizing with some designed molecules like amphiphilic molecules, polyelectrolyte polymers, polar organic solvents, and ionic liquids *etc.*,[5] which prevented the aggregation of the graphene sheets. While in the second strategy, the rGO sheets were obtained by solvothermally reducing GO in an organic solvent.[6] Under this circumstance, the organic solvent molecules absorbing at graphene planes acted as stabilizers of graphene sheets. However, most of these procedures often require hazardous reducing agents (or lengthy solvothermal reduction), specific stabilizers, and a complicated chemical process. For these reasons, it is highly desirable to develop a low-cost, facile and efficient approach for preparing soluble rGO sheets in large quantities.

In this study, we present a novel strategy for making soluble rGO sheets "on the cheap" by adopting endogenous reducing agent and stabilizer. Different from the above-mentioned strategies, our method has several advanced features that make it particularly attractive for large-scale manufacture of soluble rGO sheets for practical applications: (1) it was economical owing to just adopting two easily available and inexpensive starting materials (GO and DMF) without adding any foreign hazardous reduced agent and stabilizer; (2) it was very simple and didn't need a complex chemical procedure; (3) rGO sheets produced in this strategy had a high reduction level and could be well dispersed in different solvents.

2. Experimental

Materials

Graphite powder was purchased from Alfa Aesar. DMF was obtained from Beijing Chemical Factory (Beijing, China) and used as received without further purification. Anodisc membrane filter (50 mm in diameter, 0.18 μm pore size) was produced from Puyuan Nano, Hefei, China.

Synthesis and device fabrication

GO was synthesized from natural graphite by a modified Hummers' method.[15] The rGO sheets were obtained by a simple one-step reduction approach. In a typical experiment, the as-synthesized graphene oxide was firstly dispersed in DMF (0.5 mg ml^{-1}) under ultrasonically treatment for 30 min, and then heated in an oil bath (153 °C) for 1 h.

[a]*State Key Laboratory of Electroanalytical Chemistry, Changchun Institute of Applied Chemistry, Chinese Academy of Sciences, Changchun, PR China. E-mail: lehuilu@ciac.jl.cn*
[b]*Graduate School, Chinese Academy of Sciences, Beijing, PR China*
[c]*Heilongjiang University, Harbin, 150080, PR China*
† Electronic supplementary information (ESI) available: Fig. S1–S1 and Table S1. See DOI: 10.1039/c0jm02865g

Uniform rGO paper was prepared by vacuum filtration of the rGO dispersion through an Anodisc membrane filter, the GO paper was obtained under the same protocol.[16]

For the preparation of the gas sensing device, the as-synthesized rGO solution in DMF was filtrated, followed by drying in air and grinding. Several drops of terpineol were then added, the resulting viscous solution was directly coated on an alumina ceramic tube, dried, and finally welded on the base.

Instruments and measurements

TEM images were taken by using a TECNAI G2 high-resolution transmission electron microscope. AFM images were obtained with a microscope (Seiko Instruments Industry Co., Tokyo, Japan). The cross-sectional SEM image of rGO paper was taken with a FEI/Philips XL30 ESEM FEG field-emission scanning electron microscope operating at an acceleration voltage of 20 kV. UV/Vis spectra were recorded on a VARIAN CARY 50 UV/Vis spectrophotometer. NMR analyses were carried out on a Varian Infinityplus 400 spectrometer operating at a magnetic field strength of 9.4 T. XRD patterns were collected on a D8 ADVANCE (Germany) using Cu-Kα (0.15406 nm) radiation. TGA measurements were performed by using a Perkin-Elmer TGA-2 thermogravimetric analyzer under nitrogen from room temperature to 800 °C at 10 °C min^{-1}. Raman analysis was carried out on a J-Y T64000 Raman spectrometer with 514.5 nm wavelength incident laser light. XPS measurements were conducted with a VG ESCALAB MKII spectrometer. The XPSPEAK software (Version 4.1) was used to deconvolute the narrow-scan XPS spectra of the C 1s, O 1s and N 1s of the samples, using adventitious carbon to calibrate the C1s binding energy (284.5 eV). Conductivity was measured under ambient laboratory conditions using a standard four-probe method (Suzhou Baishen SZT-2A four-probe meter). JF02E gas sensing testing system was utilized to investigate the gas sensing properties.

3. Results and discussion

Dimethylformamide (DMF) is widely used in the chemical industry due to its cost-effectiveness and high solvent power. Previous research reported that GO can form dispersions with long-term stability in DMF.[7] Moreover, DMF is a much better solvent and can be used as the source of carbon monoxide and dimethylamine originating from its decomposition at boiling point (153 °C) (Fig. 1a).[8] It is well known that carbon monoxide is a strong reducing agent, which could highly efficiently remove oxygen from many compounds. On the other hand, previous studies showed that DMF molecules were efficient stabilizers of graphene sheets.[5e,5i] Therefore, it is expected that graphite oxides can be reduced by endogenous reducing agent (CO) from DMF heated at its boiling point to produce soluble rGO sheets in large quantities (Fig. 1b).

In a typical experiment (Fig. 1c), graphite oxides were first dispersed in DMF by sonication to obtain a light brown dispersion, and then heated to 153 °C. UV-vis spectroscopy was employed to monitor the reaction. As seen in Fig. 2a, the colour of the dispersion changed gradually to black over a period of ~20 min and was maintained with a further increase of time.

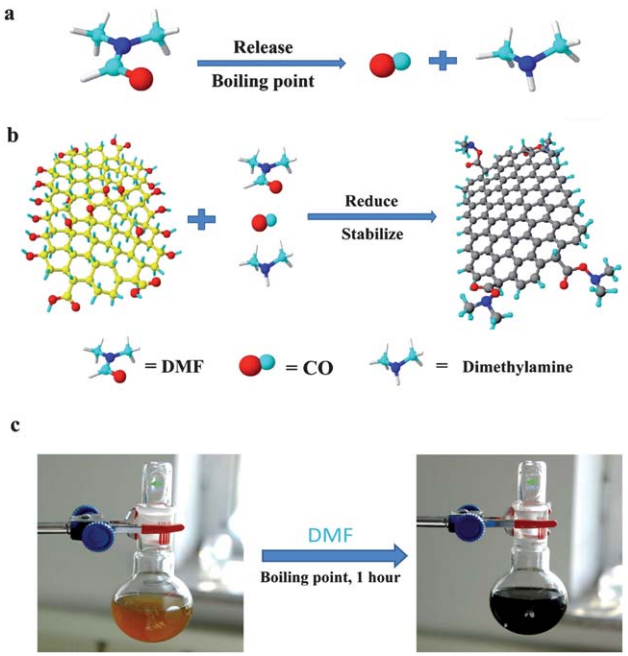

Fig. 1 (a) Decomposition of DMF upon heating at its boiling point. (b) A schematic illustration of the preparation of the rGO sheets. (c) A digital image of GO in DMF before (left) and after (right) reduction.

Meanwhile, the corresponding absorption of the dispersion increased rapidly with the reaction time and red shifted a little, signalling the conversion of graphene oxides (GO) into rGO sheets and the restoring of the electronic conjugation within the graphene sheets. Nevertheless, a tiny change in the absorption of the dispersion could be observed after one hour, revealing that the reaction was completed within one hour. In contrast, the absorption of the dispersion heated under different temperature below the boiling point of DMF increased very little with reaction time (Fig. 2b and S1†). Consequently, it was evident that temperature was a critical factor for rapidly reducing GO. In addition, no agglomerate could be observed for all of the dispersions during the heating process, suggesting that DMF could behave as an effective stabilizer for rGO sheets.

To intuitively evaluate the reduction level and determine the composition of the as-prepared rGO sheets, X-ray photoelectron spectroscopy (XPS) and ^{13}C NMR spectrum were utilized. As shown in Fig. 3a–d, the C/O ratio in the exfoliated GO increased remarkably after the reaction, and the peaks at between 286 and 289 eV which were typically assigned to epoxide, hydroxyl and carboxyl groups were significantly weakened, revealing that most of these groups were eliminated. Meanwhile, the intensity of the peak located at a binding energy of 284.4 eV (sp^2 carbon) was much enhanced compared with that of peak centered at 285.3 eV (sp^3 carbon),[2f] indicating that the as-prepared rGO had a high reduction level (Fig. 3d). Complementary to XPS data, ^{13}C NMR analysis could further confirm this result (Fig. 4). Abundant epoxide and hydroxyl groups presented in the GO sheet were mostly reduced after reaction, which is speculated to be from the significant decrease in the peak intensity at between 60–80 ppm. Importantly, the peak centered at about 130 ppm shifted to about 120 ppm and became much larger than that in the

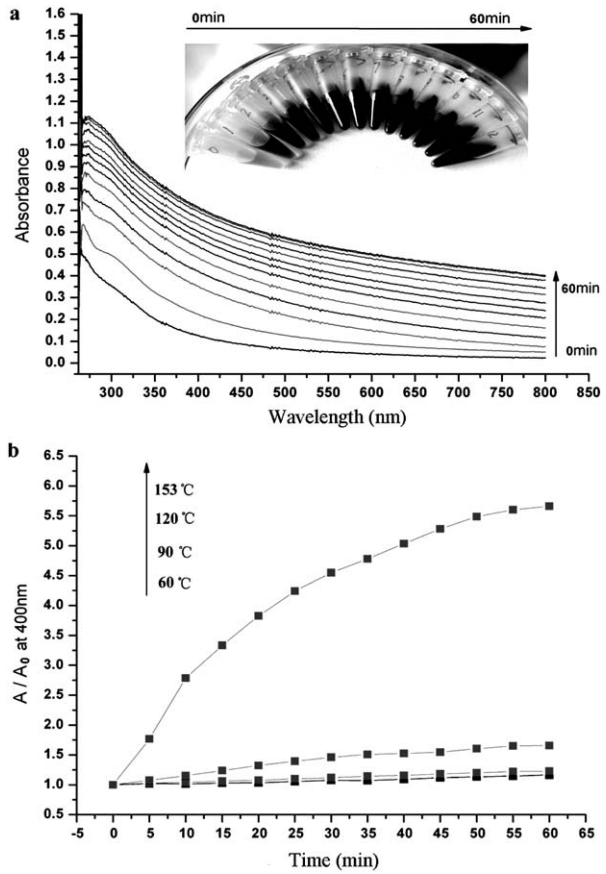

Fig. 2 (a) UV-vis absorption spectra of GO dispersions in DMF as a function of the reaction time upon heating at 153 °C (one assay per five minutes). Inset: the corresponding photographs. (b) Changes in the UV-vis absorption of GO dispersions in DMF *versus* the reaction time heated at different temperatures (from bottom to up: 60, 90, 120 and 153 °C), where A and A_0 were the absorption of the dispersions at 400 nm, respectively.

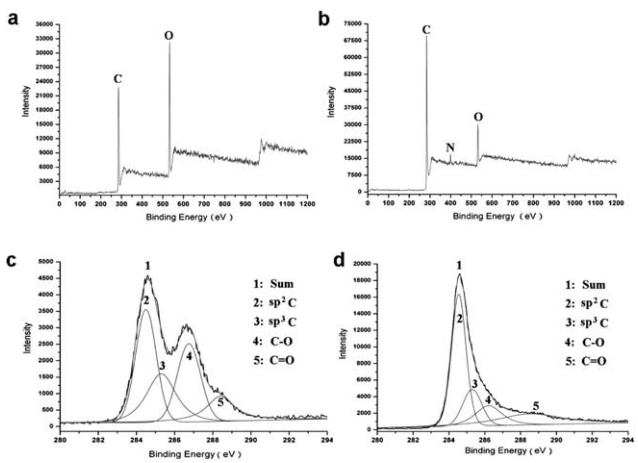

Fig. 3 Survey X-ray photoelectron spectra of the GO before (a) and after (b) reaction. (c), (d) The corresponding C1s XPS spectra.

spectrum of GO, as a result of the introduction of plentiful sp^2 carbon atoms.[5j–k,9] Also, additional two peaks located at 33.2 and 158.8 ppm, characteristic of DMF, were present, implying the absorption of DMF on the surface of the as-synthesized rGO.

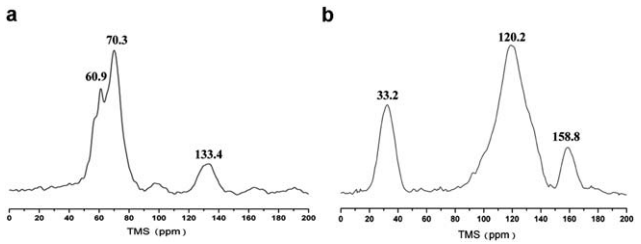

Fig. 4 The change in the ^{13}C NMR spectrum of GO (a) before and (b) after reaction.

This result could explain the presence of N in XPS and element analysis (Table S1†) as well.

Raman spectroscopy is another powerful and most widely used technique to characterize the structural and some properties of graphene such as disorder and defect structures. The G band is related to the in-plane vibration of sp^2-bonded carbon atoms, while the D band is associated with the vibrations of carbon atoms with sp^3 electronic configuration of disordered graphene. The I_D/I_G ratio of the rGO, as observed in Fig. 5, was found to be higher than that of initial GO, revealing a substantial reduction in the content of the sp^3-bonded carbon atoms and the oxidized molecular defects.[5b,f] These results, combining with X-ray powder diffraction (XRD), Fourier transform infrared (FTIR) and thermogravimetric analysis (TGA) (Fig. S2–S4 in the ESI†), which were well consistent with the XPS and ^{13}C NMR data, provided further confirmations for the formation of rGO sheets.

The high reduction level of rGO sheets synthesized by this facile method was essentially ascribed to the strong reducibility of carbon monoxide. In order to illustrate the generation of carbon monoxide in this reaction system, a typical identification experiment was designed and carried out (Fig. S5†). Firstly, a stream of argon was purged continuously through a flask with acidic litmus aqueous solution to carry the gas in this reaction system during the whole heating process, and then flowed into another flask with concentrated H_2SO_4. Finally, the gas was introduced into an aqueous solution of $PdCl_2$. It was well known that CO can selectively reduce Pd^{2+} ions into black Pd metal at room temperature.[10] As expected, black precipitates were observed in the $PdCl_2$ solution with reaction time. At the same

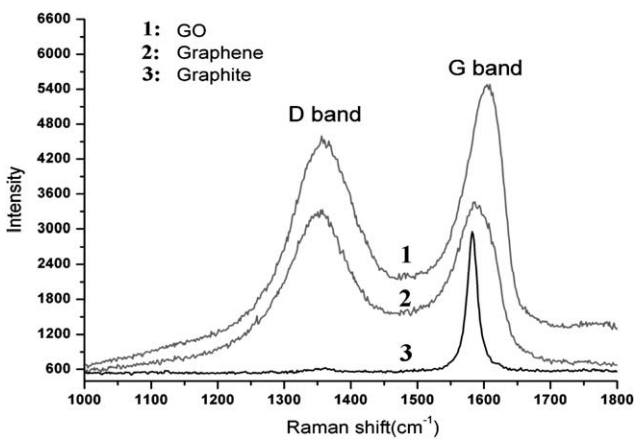

Fig. 5 Raman spectra of graphite, GO and rGO.

time, the color of litmus solution changed from red to blue due to the exposure to dimethylamine produced by the decomposition of DMF. Transmission electron microscopy (TEM) examination of the resulting black precipitates showed spherical nanostructures. From the selected-area electron diffraction analysis, all the diffraction rings were indexed to Pd metal (Fig. S6a†). Additionally, EDAX pattern manifested a strong correlation of the element with Pd metal (Fig. S6b†). Thus, it was reasonable to conclude that the formation of CO under thermal decomposition of DMF in our system enabled the reduction of GO as described in Fig. 1.

Considering the excellent dispersibility in DMF for the obtained rGO sheets, their single-sheet nature was studied using atomic force microscopy (AFM) and TEM. The cross-sectional view of AFM image showed that the average thickness of a single GO sheet was 0.89 nm. Note that the average thickness of the rGO sheet was increased a little (about 0.92 nm), which could be attributed to the capping reagents on their surface though most of the oxygen-containing functional groups were removed after the reduction. This value, however, still illuminated that the as-prepared rGO sheets remained well-separated in DMF. A similar result could be also observed in TEM image (Fig. 6b). In the case of the rGO sheets, the selected-area electron diffraction (SAED) yielded a well-defined six-fold-symmetry diffraction pattern. Furthermore, we noted that the (0–100) spots (inner hexagon) appeared to be more intense than the (1–210) spots (outer hexagon), providing a further evidence for the single-layer nature of the obtained rGO sheets.[5f,11]

It is worth pointing out that, besides DMF, the resulting rGO sheets could be easily dispersed in other solvents such as water, N-methyl-2-pyrrolidone (NMP), dimethyl- sulfoxide (DMSO), acetonitrile (ACN) and acetylacetonate (ACAC) under sonication without addition of any surfactant or other stabilizer (Fig. 7a). Such high solubility of the rGO sheets in various solvents was attributed to the stabilization of DMF absorbing on the graphene planes, since DMF is miscible with water and the majority of organic solvents. These properties are crucial to advancing many technological applications based on graphene sheets. More importantly, large-scale production of rGO sheets could be achieved by enlarging the amount of the reactant as described in Fig. 7b, revealing that this strategy has great potential for industrial production. Of particular significance was that uniform rGO paper could be readily formed by vacuum filtration of the rGO dispersion through a membrane filter. Free-standing rGO paper was acquired by peeling off the membrane after air drying. As observed in Fig. 7c, this rGO paper was bendable and exhibited a shiny metallic lustre. Scanning electron microscopy (SEM) image displayed a layer structure at the cross-section of such rGO paper (Fig. 7d). Its conductivity was found to be 6380 S m^{-1} at room temperature, which was comparable to that of rGO paper reported previously by chemical reduction method.[5c] For comparison, GO paper was also prepared under the same method. Unfortunately, it was nearly insulative. These results demonstrated that our facile and flexible reduction method could yield the rGO sheets with high conductivity and quality.

The excellent conductivity of rGO sheets discussed above, together with large surface area and strong adsorbability, incited us to investigate their great potential application as a nitrogen monoxide (NO) gas sensor. NO is an important atmospheric pollutant since NO interacts with O_2 to yield a variety of nitrogen oxides, which not only cause various serious diseases like asthma

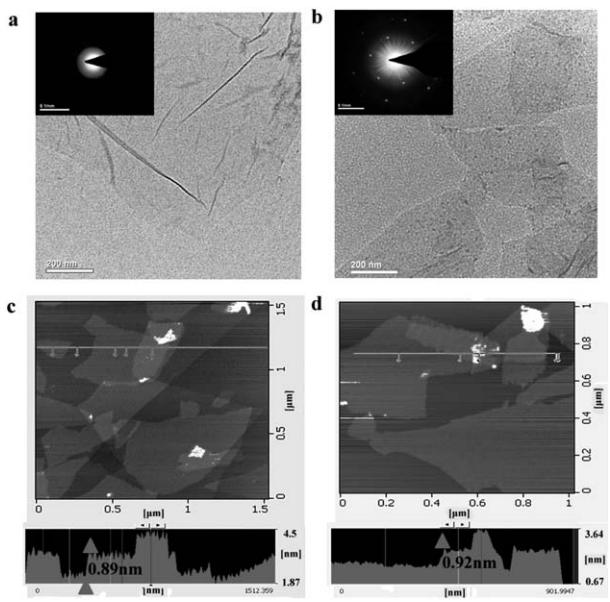

Fig. 6 Typical TEM and AFM images of GO (a,c) and the obtained rGO sheets (b,d). Insert in (a,b): the corresponding selected-area electron diffraction images.

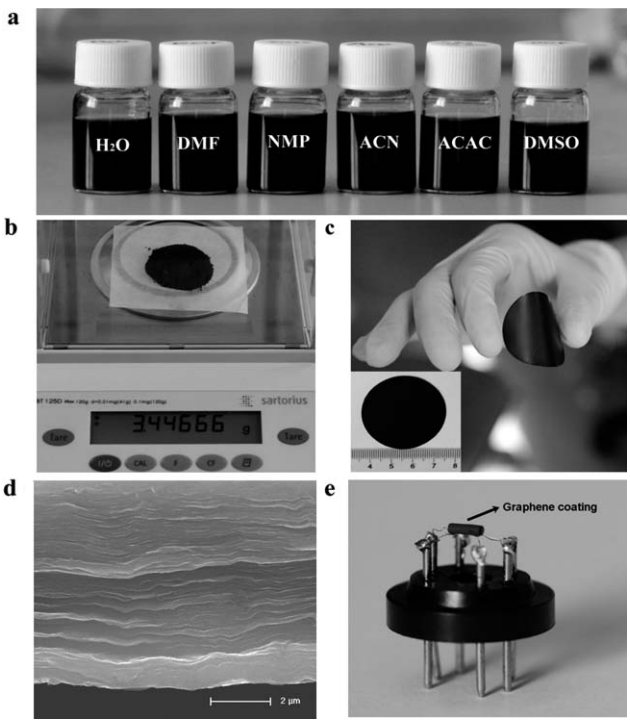

Fig. 7 (a) Dispersions of the graphene sheets in various solvents. (b) Large-scale production of the rGO sheets powder. (c) Photograph of the as-prepared rGO filtrated on an alumina membrane (d) SEM image of the cross-section of the as-prepared rGO paper. (e) Digital images of the rGO-based gas sensor device.

and carcinogenesis, but also bring destructive acid rain to the environment.[12] Moreover, it is also an important signaling molecule involved in many physiological and pathological processes within body of mammals.[13] Therefore, it is highly desirable to develop efficient sensing devices for detecting NO gas with high sensitivity and specificity. In this study, the rGO dispersion was coated on the alumina ceramic tube followed by drying in air and welding to fabricate the sensing device (Fig. 7e). The sensing performance of as-fabricated graphene-based device was characterized under practical conditions (*i.e.*, room temperature and atmospheric pressure) against various gases including NO, ethanol, acetone, NH_3, CO_2 and water vapour. Such graphene-based gas sensor exhibited high sensitivity and amazing selectivity towards NO with quite short response time and a detection limit of 0.5 ppm, a good linear correlation could be also found over the concentration range from 0.5 ppm to 15 ppm (Fig. 8). These properties endowed the rGO sheets with great potential applications in NO gas sensor. A previous study suggested that some electron-donating materials absorbing on the surface of graphene could increase the resistance of graphene.[5a] In our system, we speculated that a little dimethylamine arising from the decomposition of DMF adsorbed on the surface of the graphene and acted as an electron donator due to the lone pair electrons on the nitrogen atom, thus decreasing the conductivity of rGO. When the sensing device was exposed to NO, an electron pair acceptor, the lone pair of electrons in dimethylamine was captured, restoring the conductivity of rGO. Nevertheless, the dimethylamine-nitric oxide reaction was reversible.[14] When the device returned to air, NO was released from their surface gradually and the conductivity of rGO returned to initial value.

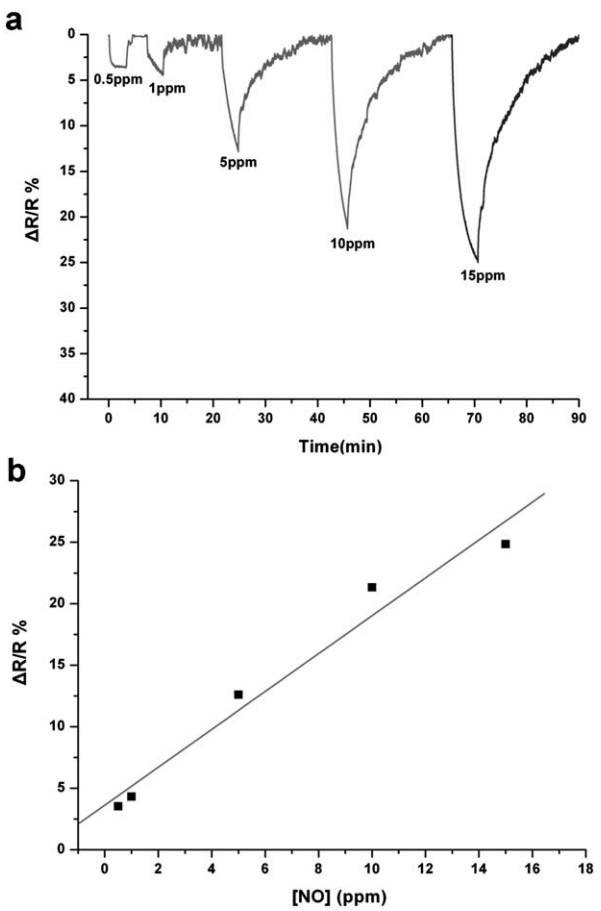

Fig. 8 (a) The sensitivity of the graphene-based gas sensing device towards nitrogen oxide. (b) The relationship between the sensitivity and the concentration of NO.

4. Conclusions

In summary, we have demonstrated a facile strategy for large-scale production of graphene sheets based on reducing the graphite oxide by carbon monoxide arising from decomposition of DMF. The crucial point of this strategy is the utilization of DMF, a widely used and cost-effective solvent. First, inexpensive starting materials should facilitate the large-scale manufacture of graphene sheets. Second, besides the capability to provide strong the reducing agent CO continuously, it can effectively stabilize the resulting graphene sheets without the need for any accessional modification procedure. Third, uniform graphene paper could be readily formed by using the as-prepared graphene sheet and exhibited high conductivity. These advantages allow this proposed synthetic approach to pave a new way for the development of high-performance graphene-based devices at low cost, as demonstrated in our preliminary study of the sensing application.

Acknowledgements

Financial support by the National Basic Research Program of China (973 Program; No.2010CB933600), the "Hundred Talents Project" of the Chinese Academy of Sciences, NSFC (No.20873138; 21075117), and State Key Laboratory of Electroanalytical Chemistry is gratefully acknowledged.

References

1 (*a*) C. H. Lui, L. Liu, K. F. Mak, G. W. Flynn and T. F. Heinz, *Nature*, 2009, **462**, 339; (*b*) F. Schedin, A. K. Geim, S. V. Morozov, E. W. Hill, P. Blake, M. I. Katsnelson and K. S. Novoselov, *Nat. Mater.*, 2007, **6**, 652; (*c*) A. K. Geim and K. S. Novoselov, *Nat. Mater.*, 2007, **6**, 183; (*d*) X. Du, I. Skachko, A. Barker and E. Y. Andrei, *Nat. Nanotechnol.*, 2008, **3**, 491; (*e*) S. Ghosh, W. Bao, D. L. Nika, S. Subrina, E. P. Pokatilov, C. N. Lau and A. A. Balandin, *Nat. Mater.*, 2010, **9**, 555; (*f*) C. N. R. Rao, A. K. Sood, K. S. Subrahmanyam and A. Govindaraj, *Angew. Chem., Int. Ed.*, 2009, **48**, 7752; (*g*) C. X. Guo, H. B. Yang, Z. M. Sheng, Z. S. Lu, Q. L. Song and C. M. Li, *Angew. Chem., Int. Ed.*, 2010, **49**, 3014; (*h*) M. J. Allen, V. C. Tung and R. B. Kaner, *Chem. Rev.*, 2010, **110**, 132; (*i*) J. Wu, W. Pisula and K. Müllen, *Chem. Rev.*, 2007, **107**, 718; (*j*) J. Kim, F. Kim and J. Huang, *Mater. Today*, 2010, **13**, 28; (*k*) X. Li, X. Wang, L. Zhang, S. Lee and H. Dai, *Science*, 2008, **319**, 1229; (*l*) M. A. Worsley, P. J. Pauzauskie, T. Y. Olson, J. Biener, J. H. Satcher and T. F. Baumann, *J. Am. Chem. Soc.*, 2010, **132**, 14067; (*m*) W. Gu, W. Zhang, X. Li, H. Zhu, J. Wei, Z. Li, Q. Shu, C. Wang, K. Wang, W. Shen, F. Kang and D. Wu, *J. Mater. Chem.*, 2009, **19**, 3367.

2 (*a*) K. S. Novoselov, D. Jiang, F. Schedin, T. J. Booth, V. V. Khotkevich and A. K. Geim, *Proc. Natl. Acad. Sci. U. S. A.*, 2005, **102**, 10451; (*b*) Y. Hernandez, V. Nicolosi, M. Lotya, F. M. Blighe, Z. Sun, S. De, I. T. Mcgovern, B. Holland, M. Byrne, Y. K. Gun'Ko, J. J. Boland, P. Niraj, G. Duesberg, S. Krishnamurthy, R. Goodhue, J. Jutchison, V. Scardaci, A. C. Ferrari and J. N. Coleman, *Nat. Nanotechnol.*, 2008, **3**, 563; (*c*) M. Choucair, P. Thordarson and J. A. Stride, *Nat. Nanotechnol.*, 2009, **4**, 30; (*d*) P. Laaksonen, M. Kainlauri, T. Laaksonen,

A. Shchepetov, H. Jiang, J. Ahopelto and M. B. Linder, *Angew. Chem., Int. Ed.*, 2010, **49**, 4946; (*e*) W. Zhang, J. Cui, C. Tao, Y. Wu, L. Ma, Y. Wen and G. Li, *Angew. Chem., Int. Ed.*, 2009, **48**, 5864; (*f*) X. Li, G. Zhang, X. Bai, X. Sun, X. Wang, E. Wang and H. Dai, *Nat. Nanotechnol.*, 2008, **3**, 538; (*g*) C. E. Hamiton, J. R. Lomeda, Z. Sun, J. M. Tour and A. R. Barron, *Nano Lett.*, 2009, **9**, 3460; (*h*) M. Lotya, Y. Hernandez, P. J. King, R. J. Smith, V. Nicolosi, L. S. Karlss, F. M. Blighe, S. De, Z. Wang, I. T. McGovern, G. S. Duesberg and J. N. Coleman, *J. Am. Chem. Soc.*, 2009, **131**, 3611.

3 (*a*) D. R. Dreyer, S. Park, C. W. Bielawski and R. S. Ruoff, *Chem. Soc. Rev.*, 2010, **39**, 228; (*b*) S. Park and R. S. Ruoff, *Nat. Nanotechnol.*, 2009, **4**, 217; (*c*) G. Eda and M. Chhowalla, *Adv. Mater.*, 2010, **22**, 2392; (*d*) L. J. Cote, R. Cruz-Silva and J. Huang, *J. Am. Chem. Soc.*, 2009, **131**, 11027.

4 (*a*) S. Stankovich, D. A. Dikin, G. H. B. Dommett, K. M. Kohlhaas, E. J. Ximney, E. A. Stach, R. D. Piner, S. T. Nguyen and R. S. Ruoff, *Nature*, 2006, **442**, 282; (*b*) N. Behabtu, J. R. Lomeda, M. J. Greem, A. L. Higginbotham, A. Sinitskii, D. V. Kosynkin, D. Tsentalovich, A. N. G. Parra-Vasquez, J. Schmidt, E. Kesselman, Y. Cohen, Y. Talmon, J. M. Tour and M. Pasquali, *Nat. Nanotechnol.*, 2010, **5**, 406.

5 (*a*) V. Dua, S. P. Surwade, S. Ammu, S. R. Agnihotra, S. Jain, K. E. Roberts, S. Park, R. S. Ruoff and S. K. Manohar, *Angew. Chem., Int. Ed.*, 2010, **49**, 2154; (*b*) V. C. Tung, M. J. Allen, Y. Yang and R. B. Kaner, *Nat. Nanotechnol.*, 2009, **4**, 25; (*c*) D. Li, M. B. Müller, S. Gilje, R. B. Kaner and G. G. Wallace, *Nat. Nanotechnol.*, 2008, **3**, 101; (*d*) Y. Xu, H. Bai, C. Li and G. Shi, *J. Am. Chem. Soc.*, 2008, **130**, 5856; (*e*) S. Park, J. An, I. Jung, R. D. Piner, S. J. An, X. Li, A. Velamakanni and R. S. Ruoff, *Nano Lett.*, 2009, **9**, 1593; (*f*) C. Zhu, S. Guo, Y. Fang and S. Dong, *ACS Nano*, 2010, **4**, 2429; (*g*) Y. Liang, D. Wu, X. Fang and K. Müllen, *Adv. Mater.*, 2009, **21**, 1679; (*h*) X. Qi, K. Pu, X. Zhu, H. Li, B. Liu, F. Boey, W. Huang and H. Zhang, *Small*, 2010, **6**, 663; (*i*) H. Yang, C. Shan, F. Li, D. Han, Q. Zhang and L. Niu, *Chem. Commun.*, 2009, 3880; (*j*) W. Gao, L. B. Alemany, L. Ci and P. M. Ajayan, *Nat. Chem.*, 2009, **1**, 403; (*k*) X. Fan, W. Peng, Y. Li, X. Li, S. Wang, G. Zhang and F. Zhang, *Adv. Mater.*, 2008, **20**, 4490.

6 (*a*) Y. Zhu, M. D. Stoller, W. Cai, A. Velamakanni, R. D. Piner, D. Chen and R. S. Ruoff, *ACS Nano*, 2010, **4**, 1227; (*b*) S. Dubin, S. Gije, K. Wang, V. C. Tung, K. Cha, A. S. Hall, K. Farrar, R. Varshneya, Y. Yang and R. B. Kaner, *ACS Nano*, 2010, **4**, 3845.

7 J. I. Paredes, S. Villar-Rodil, A. Martínez-Alonso and J. M. D. Tascón, *Langmuir*, 2008, **24**, 10560.

8 (*a*) J. Muzart, *Tetrahedron*, 2009, **65**, 8313; (*b*) Y. Wan, M. Alterman, M. Larhed and A. Hallberg, *J. Org. Chem.*, 2002, **67**, 6232.

9 (*a*) W. Cai, R. D. Piner, F. J. Stadermann, S. Park, M. A. Shaibat, Y. Ishii, D. Yang, A. Velamakanni, S. J. An, M. Stoller, J. An, D. Chen and R. S. Ruoff, *Science*, 2008, **321**, 1815; (*b*) L. B. Casabianca, M. A. Shaibat, W. W. Cai, S. Park, R. Piner, R. S. Ruoff and Y. Ishii, *J. Am. Chem. Soc.*, 2010, **132**, 5672.

10 Z. Li, Q. Sun and M. Gao, *Angew. Chem., Int. Ed.*, 2005, **44**, 123.

11 (*a*) A. C. Ferrari, J. C. Meyer, V. Scardaci, C. Casiraghi, M. Lazzeri, F. Mauri, S. Piscanec and D. Jiang, *Phys. Rev. Lett.*, 2006, **97**, 187401; (*b*) J. C. Meyer, A. K. Geim, M. I. Katsnelson, K. S. Novoselov, T. J. Booth and S. Roth, *Nature*, 2007, **446**, 60.

12 T. Yamada, H. Zhou, H. Uchida, M. Tomita, Y. Ueno, T. Ichino, I. Honma, K. Asai and T. Katsube, *Adv. Mater.*, 2002, **14**, 812.

13 T. Nagano and T. Yashimura, *Chem. Rev.*, 2002, **102**, 1235.

14 (*a*) R. S. Drago and B. R. Karstetter, *J. Am. Chem. Soc.*, 1961, **83**, 1819; (*b*) D. S. Bohle and K. N. Smith, *Inorg. Chem.*, 2008, **47**, 3925.

15 (*a*) S. Guo, D. Wen, Y. Zhai, S. Dong and E. Wang, *ACS Nano*, 2010, **4**, 3959; (*b*) W. S. Hummers Jr and R. E. Offeman, *J. Am. Chem. Soc.*, 1958, **80**, 1339.

16 D. A. Dikin, S. Stankovich, E. J. Ximney, R. D. Piner, G. H. B. Dommett, G. Evmenenko, S. T. Nguyen and R. S. Ruoff, *Nature*, 2007, **448**, 457.

